The Raman spectrum of ferroelectric PbTiO3

Autor(en): **Frey, R.A. / Silberman, E.**

Objekttyp: **Article**

Zeitschrift: **Helvetica Physica Acta**

Band (Jahr): **49 (1976)**

Heft 1

PDF erstellt am: **09.08.2024**

Persistenter Link: https://doi.org/10.5169/seals-114755

Helvetica Physica Acta, Vol. 49 (1976), Birkhäuser Verlag, Basel

The Raman Spectrum of Ferroelectric $PbTiO_3$

by **R. A. Frey**[1]) and **E. Silberman**

Physics Department, Fisk University, Nashville, Tennessee 37203

(1. VII. 75)

Abstract. Raman scattering in ferroelectric single domain crystal $PbTiO_3$ reveals 14 phonons, which can readily be assigned to $k = 0$ phonons in the crystal class C_{4v}. In addition, seven quasi-phonons can be observed. This set of phonons allows the calculation of the non-observed E(LO3) phonon, a qualitative assessment of the action of long range and short range forces in the crystal as well as the calculation of a new set of dielectric constants. The ferroelectric phase has been found to persist down to 77 K.

The Raman spectrum of single crystal $PbTiO_3$ in its ferroelectric phase was investigated. A total of 14 phonons can be observed at room temperature with various scattering geometries; all can be readily assigned to $k = 0$ phonons in the crystal class C_{4v}. In addition, seven 45° quasi-phonons have been observed. They follow closely an equation given by Merten. With the help of this equation, the Raman shift of the only non-observed E(LO3) phonon can be calculated to be at 723 cm^{-1}. Observed A_1–E and TO–LO splittings suggest that short range and long range forces have a comparable influence on phonon energies, but the polarization character of the phonons appears to be predominantly determined by long range electrostatic forces. In search for new phase transitions, the Raman spectrum was thoroughly investigated down to 77 K. No qualitative spectral changes were observed, however, which could indicate a phase transition. Finally, using the general Lyddane–Sachs–Teller relation and the observed phonon energies, the static dielectric constants $\epsilon_\parallel$ and $\epsilon_\perp$ are calculated to be 30.4 and 126 respectively.

Introduction

To date only a few lattice dynamical investigations have been performed on ferroelectric lead titanate, a most interesting member of the perovskite family, although its ferroelectric properties have been known for more than twenty years [1]. Cochran's soft phonon concept for phase transitions [2] has stimulated the search for soft phonons, particularly in $SrTiO_3$ and $BaTiO_3$. Although $PbTiO_3$ is a very interesting material, due to its large tetragonal distortion $c/a = 1.063$, experimental data have been lacking due to the great difficulty in obtaining good single domain crystals of this material.

Previous experimental investigations of the phonon spectrum of $PbTiO_3$ include

[1]) Present address: Contraves AG, Dept. ETB, 8052 Zurich, Switzerland.

infrared transmission and reflectance measurements of the powder and single crystal specimens [3, 4], Raman scattering in multi-domain [4] and single-domain [5–7] crystals, and inelastic neutron scattering in $PbTiO_3$ in the cubic and tetragonal phases [8]. Most of the first order Raman phonons have been observed in the ferroelectric phase at room temperature, but some of the assignments remain controversial. Moreover, the assessment of the role of short range and long range forces in the crystal, based on observed phonon splittings, is contradictory [4, 6, 7].

The aim of this paper is to add support to one of the previously suggested phonon assignments [6], by the use of observed quasi-phonons, and to elucidate the influence of short range and long range forces on the phonon splittings and polarizations.

Phonon Species in $PbTiO_3$

The following discussion is restricted to phonons with wave vector $k = 0$. This is generally a good approximation for phonons involved in right angle and backward Raman scattering, which are the ones we have measured in this investigation.

The classification of the $PbTiO_3$ phonons may best be seen in Figure 1. In the cubic phase there should be $3F_{1u} + 1F_{2u}$ phonons, with the F_{1u} phonons being infrared active but none being Raman active in the first order. In the tetragonal class all phonons become Raman active and all but the B_1 phonon are infrared active. Further splitting may be expected due to the action of the electric field associated with

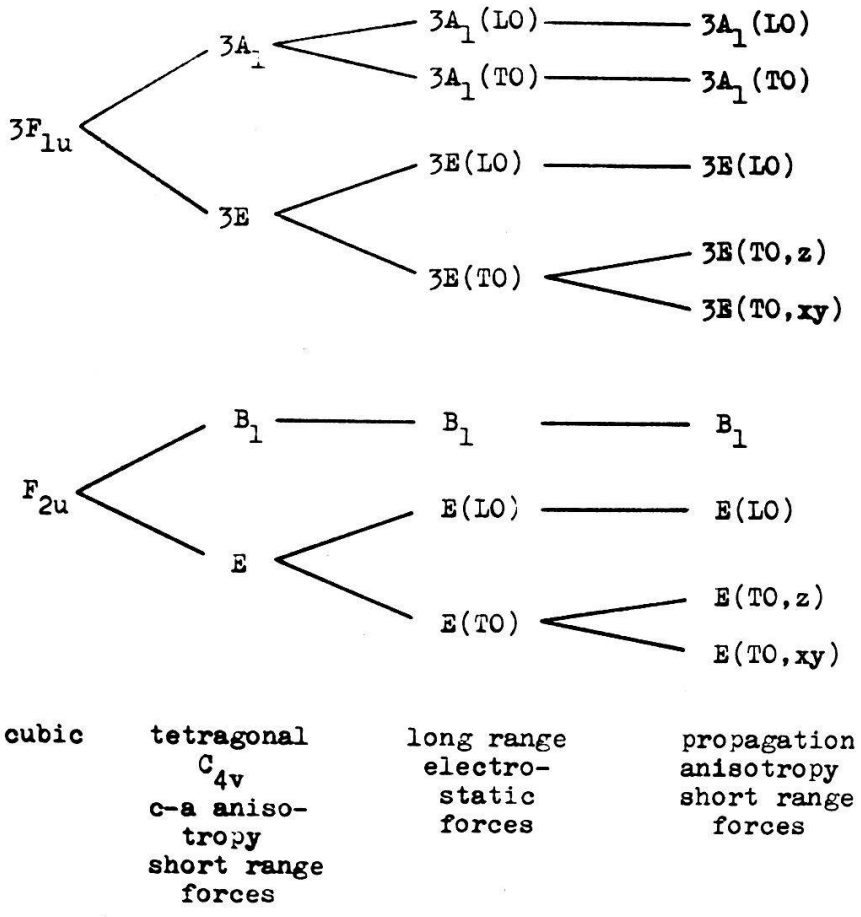

Figure 1
Splitting of optical phonons in tetragonal $PbTiO_3$ for $k = 0$.

the longitudinal infrared active phonons [9], which lifts the energy of the longitudinal phonon above that of the transverse one according to the Lyddane–Sachs–Teller relation [10]. The B_1 phonon, which carries no electric dipole moment, is not subject to such interaction. Lastly, the anisotropy of the short range forces may cause the E(TO) phonons to have different energies for propagation along the z axis or perpendicular to it. Phonons from the zone center, however, are not affected by this anisotropy. Thus, if the $k = 0$ hypothesis is a good approximation for $PbTiO_3$, a total of 15 different phonons, with symmetry species distributed according to column 3 in Figure 1 should be expected. Deviations due to the failure of the $k = 0$ assumption should show up particularly as propagational anisotropies of the E(TO) phonons because of the large tetragonal distortion c/a in $PbTiO_3$.

Experimental

The sample source and preparation have been described elsewhere [6].[2]) It should be mentioned here that the lead titanate crystals contained 0.1% of uranium in order to reduce their conductivity for dielectric measurement purposes.

Raman spectra were recorded on a Cary 81 spectrometer using 70 mW of He–Ne laser excitation. The instrument was slightly modified to allow 90° scattering also. The spectra shown in Figures 2 and 4 are original traces, recorded with a spectral slit width of 4 cm^{-1}.

Raman Spectra

For specification of the geometrical arrangement of the crystal with respect to the direction and polarization of the incident and scattered light the notation of Damen et al. is used [11].

E-*Phonons*

The E-phonon spectra have been reported previously [6] and are not reproduced here. Observed Raman shifts are given in Table I, which also contains experimental results from other sources. All expected E(TO) phonons have been observed, and they show a complete directional degeneracy. The fact that their energies are insensitive to the direction of propagation has been experimentally checked for phonons propagating along the z axis, at an angle of 45°, and perpendicular to it. There are two possible interpretations of this observation: (1) the anisotropy in the short range forces is too small to separate the phonons propagating along and perpendicular to the z axis; this seems rather surprising in view of the large c/a ratio; (2) all the observed E(TO) phonons originate from the Brillouin zone center, where E(TO, z) and E(TO, xy) phonons are degenerate; this explanation is more plausible and supports the classification of the phonons in the tetragonal class C_{4v}.

The $x(zx)y$ spectrum shows the four E(TO) phonons plus three additional, relatively weak, lines. We will try to assign them by using arguments similar to the ones put forward by Loudon [12] and by Argüello et al. [13] in their discussion of the general

---

[2]) The authors are gratefully indebted to J. P. Remeika for supplying them with single crystal samples of $PbTiO_3$.

Table I
Phonon energies in tetragonal $PbTiO_3$ and $BaTiO_3$ (cm^{-1})

	$PbTiO_3$					$BaTiO_3$
	Raman			Infrared	Neutr. scatt.	Raman
C_{4v}	Quasi-phonons	Phonons	Ref. 7	Ref. 4	Ref. 8	Ref. 15
E(TO1)		88	89	119	97	36[b])
	109					
A_1(TO1)		147	127[a])	162	148	180[c])
E(LO1)		128	128	128		715
	161					
A_1(LO1)		189	215[a])	180		727
E(TO2)		220	220	256 272		180
	310					
A_1(TO2)		359	364	355		180
E(LO2)		439	445	439 450		180
	451					
A_1(LO2)		465	445			178
E(TO3)		505	508	512 540		486 518
	559					
A_1(TO3)		646	651	614		470
E(LO3)		723[a])	717[a])	679 687		463
	773					
A_1(LO3)		796	797	790		470
E(TO4 + LO4) + B_1	289	289	290	294		305

[a]) Calculated from quasi-modes using equation (2).
[b]) True line position after correction for damping.
[c]) Calculated from the Lyddane–Sachs–Teller relation.

features of phonon spectra of uniaxial crystals with either long range or short range dominant forces.

Phonons propagating in the xy plane at 45° to the x axis and having a polarization component parallel to the x axis would contribute to the $x(zx)y$ spectrum. If short range forces would dominate in the crystal, the phonons would be polarized predominantly along the crystallographic axes irrespective of their direction of propagation. The spectrum would then show four lines due to phonons with polarization parallel to the x axis, and with Raman shifts lying between those of the corresponding E(TO) and E(LO) phonons. However, the spectrum shows four lines at exactly the E(TO) positions. Even if one assumes a vanishing E(TO)–E(LO) splitting for all E phonons, the short range force hypothesis could not account for the three additional lines in the spectrum. In the limiting case of the long range forces being dominant, the phonons would always be predominantly longitudinal or transversal, irrespective of their direction of propagation. Both E(TO) and E(LO) phonons propagating in the xy

plane at 45° to the x axis would have a polarization component in the x direction and could therefore contribute to the spectrum. This is fully consistent with the observations, and the additional lines at 439, 289 and 128 cm^{-1} must therefore be assigned to E(LO) phonons. None of the remaining weak features in the spectrum can be assigned to the fourth E(LO) phonon.

A_1-*Phonons*

The $\bar{x}(zz)x$, $\bar{y}(xx)y$ and $\bar{z}(yy)z$ spectra, showing the A_1-phonons, have been reported elsewhere [6]. Phonon frequencies obtained from these spectra are compiled in Table I.

The assignment of the A_1 spectra does not present any serious difficulties since the extra weak bands can readily be identified with the well known E(TO) phonons in most cases. It is interesting to note at this point that in all the spectra where the phonons derived from the F_{2u} mode are allowed, namely in the $\bar{y}(xx)y$ and $\bar{z}(yy)z$ scattering configurations, a prominent band appears at 289 cm^{-1}. This suggests that the E(TO), E(LO) and B_1 phonons derived from F_{2u} are all degenerate. The same observation has been made in $BaTiO_3$ [14, 15].

Quasi-Phonons

Spectrum A of Figure 2 shows phonons propagating in the xz plane at an angle of 45° to the z axis and with a polarization vector component parallel to it. Such

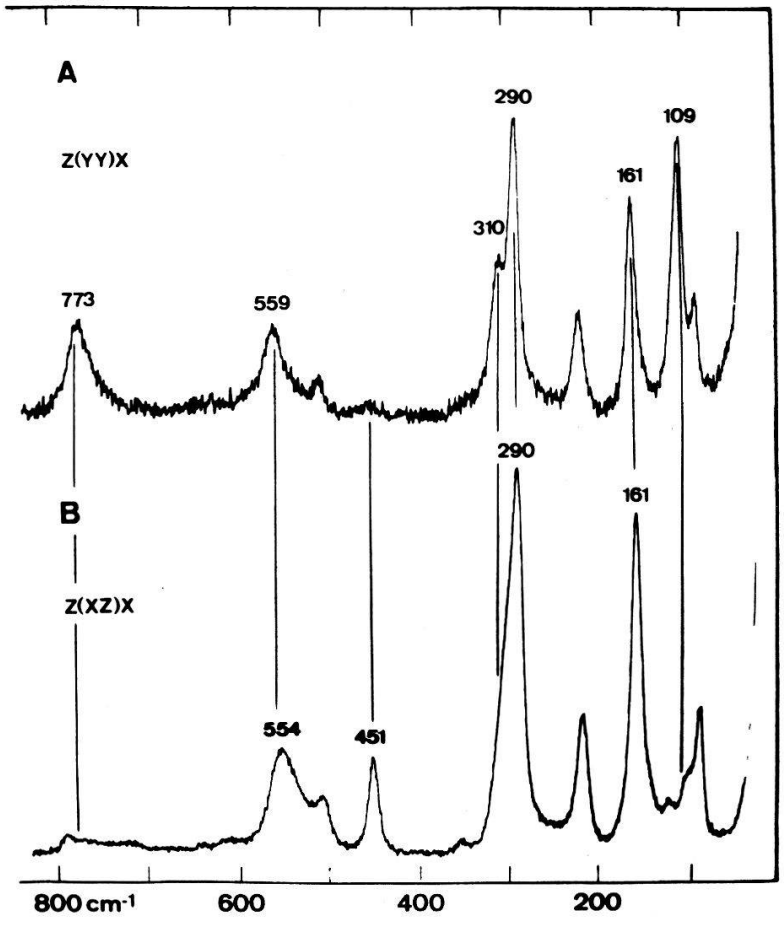

Figure 2
Transverse and longitudinal quasi-phonons in $PbTiO_3$. (A) α_{yy} scattering; (B) α_{xz} scattering.

phonons can exist only if: (1) they do not have pure symmetries A_1 or E or, (2) they are not pure TO or LO phonons. Assuming short range forces dominating in the crystal, spectrum A would be due to phonons polarized along the z axis. These phonons are termed quasi LO–TO phonons of symmetry A_1. Three such phonons should show up in the spectrum with Raman shifts lying between those of the corresponding A_1(TO) and A_1(LO) phonons. The B_1 phonon may also contribute to the spectrum with a line near 289 cm^{-1}. Spectrum B should similarly show quasi LO–TO phonons of symmetry E. Again, a total of four lines should be observed, but at definitely different locations than those of spectrum A, due to the A_1–E splitting. Subtracting the contributions from the E(TO) phonons in both spectra, six quasi-phonons can be identified in spectrum A. This is in contradiction with the assumption of dominating short range forces, which can only account for four lines in each (of both) spectra. In addition, the quasi-phonons in both spectra do not appear at different positions, but each line assigned in either spectrum to a quasi-phonon is present in the other spectrum at the same position, although with modified intensity in some cases. One is therefore led to give up the concept of dominating short range forces and to assume that the phonon polarization is essentially determined by the long range forces. For, in such a case, transverse and longitudinal phonons propagating in the xz plane at 45° to the z axis and with the polarization vector lying in the xz plane would have non-vanishing polarization components along the x and z directions and would contribute to both A and B spectra. Consequently, spectra A and B should be identical as far as peak positions are concerned, which is consistent with the observations. The differences of line intensities in both spectra are due to the fact that different components of the polarizability tensor, namely α_{yy} and α_{xz}, are responsible for the appearance of the respective lines. From each F_u phonon in the cubic phase, two quasi-phonons may be derived in the tetragonal phase. Considering the degeneration of all phonons derived from F_{2u}, a total of seven quasi-modes should be present in the spectra. This is in fact the total number of lines assigned to quasi-phonons in both spectra. In all, the consistency of the hypothesis of dominating long range forces with observed Raman spectra suggests strongly that the polarization of the infrared active phonons in $PbTiO_3$ is determined predominantly by the interaction of long range Coulomb type forces with the ions. The observed Raman shifts for the quasi-phonons are given in Table I.

Discussion

The forces which act in an ionic crystal, such as the ferroelectric perovskites, may be roughly classified into long range and short range forces. The long range forces are of the Coulomb type, while the short range forces arise from the overlapping of the electron clouds of the ions and are of the repulsive type. The anisotropy of the latter is due to the tetragonal distortion of these crystals and is reflected in the A_1–E phonon splitting. Likewise, the TO–LO splitting reflects the action of the electric field associated with the longitudinal infrared active phonons on the ions. This interaction of electric fields with lattice vibrations is expressed in the generalized Lyddane–Sachs–Teller relations [16]

$$\prod_i \frac{\omega_{A_1}(LO_i)}{\omega_{A_1}(TO_i)} = \left(\frac{\epsilon_\parallel^0}{\epsilon_\parallel}\right)^{1/2}; \quad \prod_i \frac{\omega_E(LO_i)}{\omega_E(TO_i)} = \left(\frac{\epsilon_\perp^0}{\epsilon_\perp}\right)^{1/2}. \tag{1}$$

Merten [17][3]) has derived a formula which relates the frequency ω of quasi-phonons in uniaxial crystals to the clamped high frequency dielectric constants $\epsilon_\parallel$ and $\epsilon_\perp$ and to the frequency of the A_1(TO–LO) and E(TO–LO) phonons:

$$\epsilon_\parallel \cos^2\theta \prod_{i=1}^{n} [\omega^2_{A_1}(LO_i) - \omega^2] \prod_{i=1}^{m} [\omega^2_{E}(TO_i) - \omega^2]$$

$$+ \epsilon_\perp \sin^2\theta \prod_{i=1}^{m} [\omega^2_{E}(LO_i) - \omega^2] \prod_{i=1}^{n} [\omega^2_{A_1}(TO_i) - \omega^2] = 0 \qquad (2)$$

where θ is the angle between the z axis and the direction of phonon propagation.

The values of $\epsilon_\parallel = 7.211$ and $\epsilon_\perp = 7.270$ for Na light can be obtained from the optical data of Shirane et al. [18], and Singh et al. [19]. Equation (2), however, depends on the ratio $\epsilon_\parallel/\epsilon_\perp$ only. As one can further see from equation (2), the quasi-phonons merge with the A_1(LO) and E(TO) phonons as θ approaches 0°. For phonons propagating perpendicular to the z axis, the roots of equation (2) correspond to the A_1(TO) and E(LO) phonons. Since the phonons derived from the F_{2u} branch are all degenerate, including the corresponding quasi-phonons, they do not contribute to equation (2). We have then $m = n = 3$. Substituting the highest observed quasi-mode, which has to be a longitudinal quasi A_1–E phonon, into equation (2) one obtains 723 cm^{-1} for the highest nonobserved E(LO) phonon. This value is also included in Table I. To further support this calculated value for E(LO3) and to test the validity of Merten's equation, the directional dispersion of the quasi-phonons calculated for $\theta = 45°$ should reproduce the observed quasi-phonons. These dispersion curves are displayed in Figure 3. The quasi-phonon frequencies observed at 45° are indicated by squares in the figure and are listed in Table I. The calculated quasi-phonon frequencies are 114, 159, 310, 450, 561 and 773 cm^{-1}. The agreement is quite good, particularly in the high frequency region. Thus the calculated value for E(LO3) is very probably quite close to the real value.

We return now to Table I for comparison of experimental results with previous Raman work. Burns et al. [7] have calculated the A_1(TO1) and A_1(LO1) phonons using equation (2) and observed the E(TO1) and E(LO1) phonons and the quasi-phonons at 109 and 161 cm^{-1}. The assignment of the weak line at 187 cm^{-1} to the A_1(LO1) phonon reported earlier [6] seems to be sufficiently established and it also correlates nicely with the quasi-mode at 161 cm^{-1} (cf. Fig. 3).

Burns et al. [7] assigned the line at 147 cm^{-1} to a second order effect. Our arguments for assigning the 147 cm^{-1} band to the A_1(TO1) phonon may be summarized as follows:

(i) The 147 cm^{-1} band is a very prominent line in the A_1(TO) spectra with a half width comparable with other bands. It does not show the temperature dependence of the intensity typical for second order bands and remains a prominent spectral feature at 77 K.

(ii) Infrared reflectance measurements [4] and neutron diffraction data [8] are in good agreement with the suggested assignment.

(iii) Substituting the quasi-phonon at 161 cm^{-1} into equation (2) yields 150 cm^{-1} for the A_1(TO1) phonon, which is in good agreement with observation.

The general accordance of Raman data with infrared reflectance data [4] is fair,

---

[3]) The authors wish to thank Dr. J. F. Scott for having drawn their attention to this article.

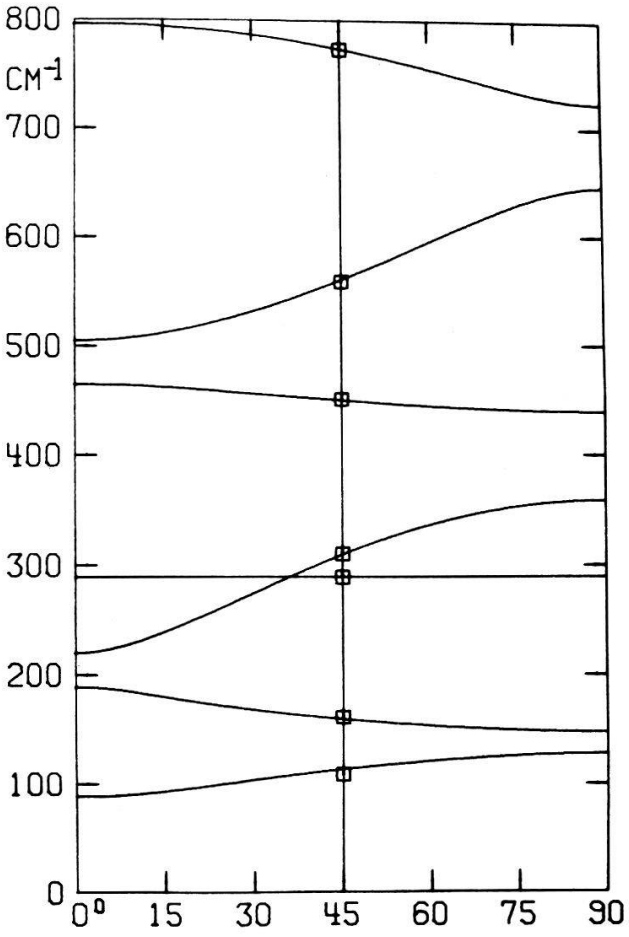

Figure 3
Directional dispersion of phonons in $PbTiO_3$. The abscissa indicates the angle between the tetragonal axis and the direction of phonon propagation. Measured values at 45° are indicated by small squares.

considering the approximations necessary to perform the Kramers–Kronig analysis. The assignment of the different F_{1u} phonons to their respective branches has some difficulties and it cannot be completed unambiguously. However, the correspondence between each TO–LO phonon pair becomes unique if one assumes that every LO phonon has a higher energy than the corresponding TO phonon, as it is strongly suggested by the generalized LST relation (cf. Eq. (1)). For comparison purposes it may be useful to look at the situation of $BaTiO_3$, although the case seems to be even less clear than the one of $PbTiO_3$. In the most recent communications on the Raman spectrum of $BaTiO_3$, a set of lines essentially similar to the ones of $PbTiO_3$ has been assigned to first order Raman bands [14, 15] but their symmetry specification is not completely clear. Moreover, there is no consistency at all in the assignment of the phonons to the three F_{1u} branches. This can be seen in Table I where we have reproduced the results of the work on $BaTiO_3$ carried on by Di Domenico et al. [15]. The main features of this work are that the phonons derived from the F_{2u} branch are all degenerate, as in $PbTiO_3$, and that the phonons derived from the second and third F_{1u} branch are nearly degenerate. For the E(TO3) phonon a propagational anisotropy has been observed: the E(TO3, z) and E(TO3, xy) phonons appear at 518 and 468 cm^{-1}, respectively. No such anisotropy has been observed in $PbTiO_3$. The large TO–LO splitting in the first branch of $BaTiO_3$ is very peculiar and has no analogy in $PbTiO_3$.

The lowest transverse mode has been calculated as the true position of the soft mode using the data of a strongly damped mode which appears near the exciting line. Evidently, careful investigation of the phonon spectra near the transition point, together with information on the cubic phase which can be obtained from neutron scattering, would facilitate the assignment of the phonons to the different F_{1u} branches.

Dielectric Constants

The dielectric constants in solids are related to the lattice vibrational modes through the generalized Lyddane–Sachs–Teller relations shown in equation (1). These equations hold for the clamped dielectric constants and for undamped phonons near the zone center, but still away from the polariton dispersion region. All these conditions are fulfilled for $PbTiO_3$. Measurements of the high frequency refractive indices have been published by Singh et al. [19] and yield a birefringence of $\Delta n = n_a - n_c = 0.0116$ for Na light. This is in good agreement with $\Delta n = 0.011$ reported earlier by Shirane et al. [18]. In the only investigation on the static dielectric constants of single domain $PbTiO_3$ a value of $\epsilon_{\parallel}^0 = 30$ was reported [20]. No value for $\epsilon_{\perp}^0$ was given, probably because the platelet-shaped crystals were *c*-domain crystals and did not allow any measurement of $\epsilon_{\perp}^0$. We now return to equation (1) to calculate the static dielectric constants. Using $\epsilon_{\parallel} = 7.211$ and $\epsilon_{\perp} = 7.270$ (cf. Discussion) and the phonon energies from Table I one obtains for the static dielectric constants of $PbTiO_3$ $\epsilon_{\parallel}^0 = 30.4$ and $\epsilon_{\perp}^0 = 125.6$. The corresponding values for $BaTiO_3$, calculated with the phonon frequencies listed in Table I, are 80 and 1950, respectively. The differences between $PbTiO_3$ and $BaTiO_3$ are striking, particularly in $\epsilon_{\perp}^0$. The high static dielectric constant perpendicular to the *c* axis in $BaTiO_3$ results from the fact that the lowest E(TO) phonon is very soft even far away from the transition point, while in $PbTiO_3$ the corresponding phonon is much harder.

Phase Transitions

Because the high temperature region has already been investigated extensively [3–5, 7, 8] we have paid particular attention to the low temperature region. The question of low temperature phase transitions is highly relevant because $BaTiO_3$, for example, is known to have two more ferroelectric phases below the tetragonal phase. In addition, due to the fact that $PbZrO_3$ is antiferroelectric, it is conceivable that $PbTiO_3$ may become antiferroelectric at low temperature. From dielectric constant measurements, Kobayashi et al. have reported two phase transitions in the powder at $-100°$ and $-150°$C. The transition at $-100°$C was also observed by X-ray measurements [21]. The change in the X-ray pattern was tentatively interpreted as a transition to an antiferroelectric phase with $a' = 4a$ and $c' = 2c$, where *a* and *c* are the tetragonal lattice parameters. No information about the character of the low temperature transitions has been reported. The marked thermal hysteresis of the transitions required a cooling rate of approximately 0.3°C/min.

The Raman spectra of a single crystal of $PbTiO_3$, cooled to $-110°$C at rates not exceeding 0.3°C/min and subsequently cooled rapidly to 77 K, was recorded for various scattering geometries. Figure 4 reproduces the E phonon spectra at room temperature and at 77 K after following the described cooling procedure. The E phonon spectrum should be the most sensitive with respect to phase changes since the strong line intensities permit the use of a resolution of 0.8 cm^{-1}. The result of this

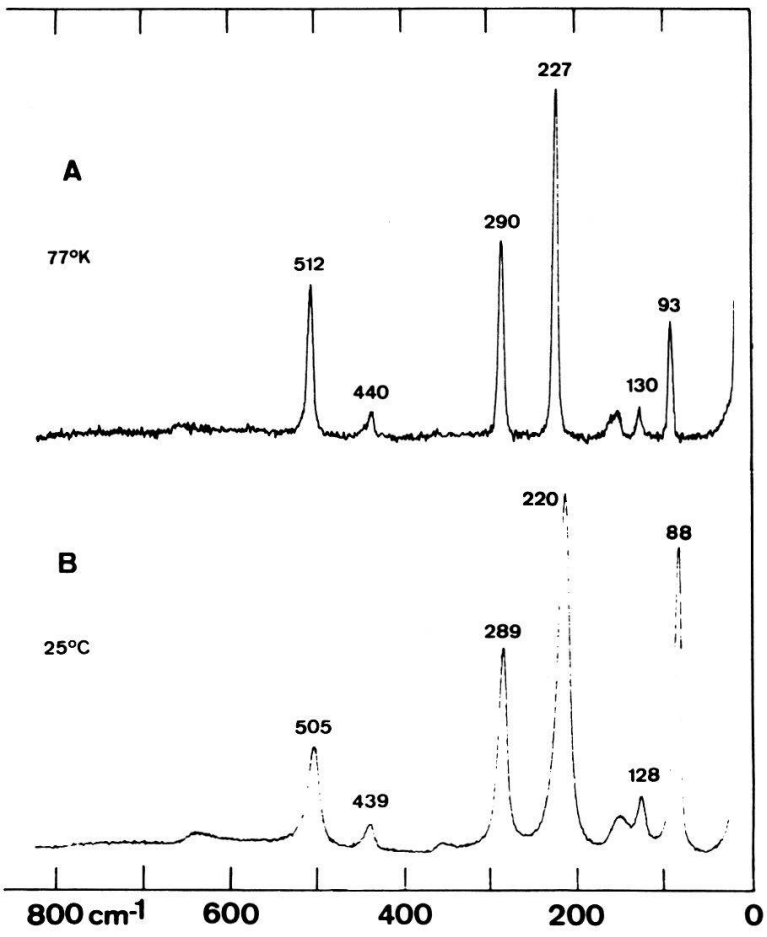

Figure 4
Transverse and longitudinal optical phonons in $PbTiO_3$. (A) At 77 K; (B) at room temperature.

investigation is negative. The low temperature spectrum does not show any new lines nor does it reveal splittings of the E phonons. The quantitative changes in the spectra, such as peak intensity, line width and position depend continuously on the temperature. Moreover, spectrum A in Figure 4 does not differ in any respect from the spectrum of a crystal cooled rapidly from room temperature to 77 K. It is hard to accept that the appearance of any superstructure, such as suggested by Kobayashi et al. [21], would not result in any detectable spectral change. The above results suggest that the tetragonal ferroelectric phase is stable down to 77 K under the thermal treatment described above. These conclusions are however not necessarily contradictory to the data from X-ray and dielectric constants measurements, as the latter experiments were performed on the powder. It is likely that the size and shape of the small powder particles, together with the electric field of the surface charges and the completely unknown domain pattern have some influence on phase stability. On the other hand, the crystals we investigated contained uranium dopants and lattice imperfections whose influences in the structural stability are difficult to assess.

Conclusion

Table I shows that the A_1–E splitting and the TO–LO separation are of the same order. On the other hand, the spectra have been interpreted on the basis of dominating long range forces. This appears to be a contradiction. However, although the magnitude

of the A_1–E and LO–TO splittings depend solely on the magnitude of the short range or long range forces, respectively, the polarization character of the phonons result from the interplay of both forces, and this fact has been taken into account in making the assignments.

The well behaved Raman spectrum of $PbTiO_3$ suggests that further detailed Raman studies near the transition, as well as electric field induced scattering experiments in the cubic phase, might elucidate the behavior of the soft phonon in this material.

REFERENCES

[1] G. SHIRANE, S. HOSHINO and K. SUZUKI, Phys. Rev. *80*, 1105 (1950); G. A. SMOLENSKII, Doklady Akad. Nauk. SSSR *70*, 405 (1950).
[2] W. COCHRAN, Adv. Phys. *9*, 387 (1960).
[3] C. H. PERRY, B. N. KHANNA and G. RUPPRECHT, Phys. Rev. *135A*, 408 (1964).
[4] N. E. TORNBERG and C. H. PERRY, J. Chem. Phys. *53*, 2946 (1970).
[5] G. BURNS and B. A. SCOTT, Phys. Rev. Lett. *25*, 167 (1970).
[6] R. A. FREY, *Adv. in Raman Spectroscopy*, Vol. I edited by J. P. MATHIEU (Heyden and Son, Ltd., London, 1973), p. 181.
[7] G. BURNS and B. A. SCOTT, Phys. Rev. *B7*, 3088 (1973).
[8] G. SHIRANE, J. D. AXE, J. HARADA and J. P. REMEIKA, Phys. Rev. *B2*, 155 (1970).
[9] M. BORN and K. HUANG, *Dynamical Theory of Crystal Lattices*, Internat. Ser. of Monographs on Physics (Oxford University Press, 1966).
[10] R. H. LYDDANE, R. G. SACHS and E. TELLER, Phys. Rev. *59*, 673 (1941).
[11] T. C. DAMEN, S. P. S. PORTO and B. TELL, Phys. Rev. *142*, 570 (1966).
[12] R. LOUDON, Adv. Phys. *13*, 423 (1964).
[13] C. A. ARGÜELLO, D. L. ROUSSEAU and S. P. S. PORTO, Phys. Rev. *181*, 1351 (1969).
[14] A. PINCZUK, W. TAYLOR and E. BURSTEIN, Sol. State Commun. *5*, 429 (1967); L. RIMAI, J. L. PARSONS and J. T. HICKMOTT, Phys. Rev. *168*, 623 (1968).
[15] M. DIDOMENICO, JR., S. H. WEMPLE and S. P. S. PORTO, Phys. Rev. *174*, 522 (1968).
[16] W. COCHRAN and R. A. COWLEY, J. Phys. Chem. Sol. *23*, 447 (1962).
[17] L. MERTEN, Phys. Stat. Sol. *25*, 125 (1968).
[18] G. SHIRANE, R. PEPINSKY and B. C. FRAZER, Acta Cryst. *9*, 131 (1956).
[19] S. SINGH, J. P. REMEIKA and J. R. POTOPOWICZ, Appl. Phys. Lett. *20*, 135 (1972).
[20] V. G. BHIDE, K. G. DESHMUKH and M. S. HEDGE, Physica *28*, 871 (1962).
[21] J. KOBAYASHI and R. VEDA, Phys. Rev. Lett. *99*, 1900 (1955); J. KOBAYASHI, S. OKAMOTO and R. VEDA, Phys. Rev. Lett. *103*, 830 (1956).